

# Novel integral inequality approach on master–slave synchronization of chaotic delayed Lur’e systems with sampled-data feedback control

Kaibo Shi · Xinzhi Liu · Hong Zhu ·  
Shouming Zhong · Yajuan Liu · Chun Yin

Received: 23 April 2015 / Accepted: 13 September 2015 / Published online: 25 September 2015  
© Springer Science+Business Media Dordrecht 2015

**Abstract** This paper proposes a novel approach to study the problem of master–slave synchronization for chaotic delayed Lur’e systems with sampled-data feedback control. Specifically, first, it is assumed that the sampling intervals are randomly variable but bounded. By getting the utmost out of the usable information on the actual sampling pattern and the nonlinear part condition, a newly augmented Lyapunov–Krasovskii functional is constructed via a more general delay-partition approach. Second, in order to obtain less conservative synchronization criteria, a novel integral inequality is developed by the mean of the new adjustable parame-

ters. Third, a longer sampling period is achieved by using a double integral form of Wirtinger-based integral inequality. Finally, three numerical examples with simulations of Chua’s circuit are given to demonstrate the effectiveness and merits of the proposed methods.

**Keywords** Chaotic Lur’e system · Synchronization · Sampled-data control · Wirtinger-based integral inequality · Lyapunov–Krasovskii functional

## 1 Introduction

In the past few decades, chaos synchronization problem has attracted increasing attention in numerous research areas of science. This stems from the fact that synchronization problem has a wide range of applications and great potential in various dynamical systems, such as neural networks [1–3], complex networks [4–

This work was supported by National Basic Research Program of China (2010CB732501), National Natural Science Foundation of China (61273015), The National Defense Pre-Research Foundation of China (Grant No. 9140A27040213DZ02001), The Fundamental Research Funds for the Central Universities (ZYGX2014J070), The Program for New Century Excellent Talents in University (NCET-10-0097).

K. Shi (✉) · H. Zhu · C. Yin  
School of Automation Engineering, University of  
Electronic Science and Technology of China, Chengdu  
611731, China  
e-mail: skbs111@163.com

H. Zhu  
e-mail: zhuhong@uestc.edu.cn

C. Yin  
e-mail: yinchun.86416@163.com

X. Liu  
Department of Applied Mathematics, University of  
Waterloo, Waterloo, ON N2L 3G1, Canada  
e-mail: xzliu@uwaterloo.ca

X. Liu  
Department of Civil and Environmental Engineering, University  
of Waterloo, Waterloo, ON N2L 3G1, Canada

S. Zhong  
School of Mathematical Sciences, University of Electronic Sci-  
ence and Technology of China, Chengdu 611731, China  
e-mail: zhongsm@uestc.edu.cn

Y. Liu  
Department of Electronic Engineering, Daegu University,  
Gyeongsan 712-714, Republic of Korea  
e-mail: yajuan.liu.12@gmail.com

7], complex nonlinear systems [8,9], fractional-order chaotic systems [10,11], secure communication [12], PD control [13], adaptive control [14], impulsive control [15,16] and other scientific areas [17,18].

It has been noted that a large amount of nonlinear systems could be modeled accurately in the form of Lur'e control systems, such as Chua's circuit, network systems, hyper chaotic attractors and n-scroll attractor, which contain a feedback connection of a linear system and a nonlinear element satisfying the sector condition [19–23]. Therefore, the master–slave synchronization of chaotic Lur'e systems has been a very hot research topic, and a number of master–slave synchronization criteria and important methods have been proposed. For example, in [20], the global exponential synchronization problem of nonlinear time-delay Lur'e systems has been investigated via delayed impulsive control. In [21], the synchronization problem for reaction–diffusion neural networks has been discussed by using stochastic sampled-data controller. With the introduction of a delay decomposition approach, the synchronization problem of Lur'e systems with only constant time delay has been considered in [22]. In order to obtain better stability results, the problem of designing time-varying delay feedback controllers for master–slave synchronization of Lur'e systems has been addressed by employing Lyapunov–Krasovskii functional (LKF) approach in [23]. It should be noted that two cases of time-varying delays are fully considered in [23], and the gained synchronization criteria are more widespread and resultful than the ones in [17,22].

It is well known that time delay is inescapable in a large amount of physical processes [24,25]. Meanwhile, it often results in one of the main factors of poor performance or even instability [5,6,13–17,26,27]. Thus, a great deal of attention and interests has been focused on the synchronization of chaotic Lur'e systems with time delays [22,23,28–30]. Hence, many important and interesting control methods have been established for the master–slave synchronization of Lur'e systems, such as feedback control [22,23], fuzzy control [31,32], fuzzy impulsive control [33]. However, with the high-speed development of the modern high-speed computer technology, microelectronics and communication networks, the best way is to use digital controllers instead of analog circuits [28–30,33–39]. The advantage of this method lies in only needing the samples of the state variables of the master–slave

chaotic systems at discrete time instants via sampled-data controllers.

Meanwhile, how to choose the effective sampling period is very crucial to achieve chaos synchronization. Lately, based on the input delay approach [40], the sampled-data master–slave synchronization schemes have been investigated broadly in [28–30,38,39,41]. The sampled-data control problem for the master–slave synchronization is studied extensively by introducing a discontinuous LKF in [29,30,46]. Wu et al. [43] have considered the problem of sampled-data synchronization for Markovian jump neural networks with time-varying delay and variable samplings. Liu and Lee [44] have studied the synchronization problem of chaotic Lur'e systems with stochastic sampled-data control. Ge et al. [45] have investigated the robust synchronization problem of chaotic Lur'e systems with external disturbance using sampled-data  $H_\infty$  controller. In [29,30,42], in order to build improved stability conditions, a piecewise differentiable LKF is constructed. In [28], the main attention is focused on the problem of sampled-data control for master–slave synchronization of identical chaotic delayed Lur'e systems (CDLSs) by choosing a new LKF. Different from those in [29,30], the proposed LKF in [28] is positive definite at sampling times but not necessarily positive definite inside the sampling interval. However, some important and useful information of estimating the upper bound of the derivative of the LKF and nonlinear functions has not been well utilized in [28–30,44–46], which may result in the conservatism of proposed results to a certain extent. Therefore, it is an interesting and valuable issue to find a more effective approach to obtain a longer sampling period under which synchronization can be ensured theoretically.

Motivated by the issues discussed above, we consider the problem of master–slave synchronization for chaotic Lur'e systems with or without time delays by applying sampled-data feedback control in this paper. Firstly, by introducing two new adjustable parameters  $(\alpha, \beta)$ , we develop a creative integral inequality in Lemma 2, which includes Wirtinger's integral inequality and Jensen's inequality and is more tighter to estimate the bounds of the integral terms than the existing ones. Besides, for getting perfect synchronization criteria, we choose an appropriate and continuous LKF with two triple integral terms, which also takes full advantage of the available information about the actual sampling pattern. Furthermore, based on a new dou-

ble integral form of Wirtinger-based integral inequality (WBII), the desired sampling controller is achieved via solving a set of linear matrix inequalities. Finally, three numerical simulations are performed on Chua’s circuit. It is shown clearly that the proposed results are effective and can significantly improve the existing ones.

*Notation* Notations used in this paper are fairly standard:  $\mathbb{R}^n$  denotes the  $n$ -dimensional Euclidean space,  $\mathbb{R}^{n \times m}$  the set of all  $n \times m$  dimensional matrices,  $I$  the identity matrix of appropriate dimensions,  $A^T$  the matrix transposition of the matrix  $A$ . By  $X > 0$  (respectively  $X \geq 0$ ), for  $X \in \mathbb{R}^{n \times n}$ , we mean that the matrix  $X$  is real symmetric positive definite (respectively, positive semi-definite);  $\text{diag}\{r_1, r_2, \dots, r_n\}$  block diagonal matrix with diagonal elements  $r_i, i = 1, 2, \dots, n$ , the symbol  $*$  represents the elements below the main diagonal of a symmetric matrix,  $A \otimes B$  the Kronecker product of the matrices  $A$  and  $B$ ,  $A_s$  is defined as  $A_s = \frac{1}{2}(A + A^T)$ .

**2 Preliminaries**

Consider the following master–slave synchronization of CDLSs with sampled-data feedback control:

$$\mathfrak{M}: \begin{cases} \dot{x}(t) = \mathcal{A}x(t) + \mathcal{B}x(t-h) + \mathcal{W}f(\mathcal{D}x(t)), \\ \gamma(t) = \mathcal{C}x(t), \end{cases} \quad (1)$$

$$\mathfrak{S}: \begin{cases} \dot{z}(t) = \mathcal{A}z(t) + \mathcal{B}z(t-h) \\ \quad + \mathcal{W}f(\mathcal{D}z(t)) + u(t), \\ \lambda(t) = \mathcal{C}z(t), \end{cases} \quad (2)$$

$$\mathfrak{C}: u(t) = \mathcal{K}(\gamma(t_k) - \lambda(t_k)), t \in [t_k, t_{k+1}), \quad (3)$$

which consists of master system  $\mathfrak{M}$ , slave system  $\mathfrak{S}$  and controller  $\mathfrak{C}$ .  $\mathfrak{M}$  and  $\mathfrak{S}$  with  $u(t) = 0$  are identical CDLSs with state vectors  $x(t), z(t) \in \mathbb{R}^n$ , outputs of subsystems are  $\gamma(t)$  and  $\lambda(t) \in \mathbb{R}^l$ , respectively.  $u(t) \in \mathbb{R}^n$  is the slave system control input,  $\mathcal{A} \in \mathbb{R}^{n \times n}$ ,  $\mathcal{B} \in \mathbb{R}^{n \times n}$ ,  $\mathcal{W} \in \mathbb{R}^{n \times m}$ ,  $\mathcal{D} \in \mathbb{R}^{m \times n}$  and  $\mathcal{C} \in \mathbb{R}^{l \times n}$  are known real matrices,  $\mathcal{K} \in \mathbb{R}^{n \times l}$  is the sampled-data feedback control gain matrix to be designed.  $h > 0$  is the constant time delay. The block diagram for master–slave systems with a sampled-data controller is shown in Fig. 1. It is assumed that  $f(\cdot): \mathbb{R}^m \rightarrow \mathbb{R}^m$  is a nonlinear function vector with  $f_s(\cdot)$  belonging to sector  $[k_s^-, k_s^+]$  for  $s = 1, 2, \dots, m$ . Besides, the nonlinear function  $f_s(\alpha)$  is clearly shown as shaded area in Fig. 2.

For sampled-data synchronization, only discrete measurements of  $\gamma(t)$  and  $\lambda(t)$  can be used for syn-

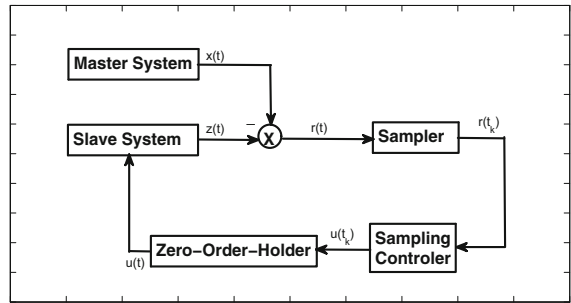


**Fig. 1** Master–slave system with a sampled-data controller

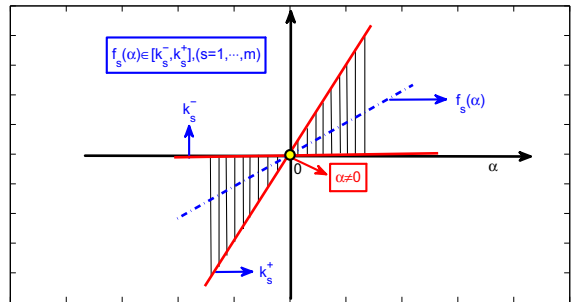


**Fig. 2** Nonlinearity characteristic with sector constraint

chronization purposes, that is, we only have the measurements  $\gamma(t_k)$  and  $\lambda(t_k)$  at the sampling instant  $t_k$ . In this paper, the control signal is assumed to be generated by using a zero-order-hold (ZOH) function with a sequence of hold times  $0 = t_0 < t_1 < \dots < t_k < \dots < \lim_{k \rightarrow \infty} t_k = +\infty$ . For the sampling interval, we impose the following assumption.

**Assumption 1** It is assumed that the interval between any two sampling instants is bounded by  $d$  ( $d > 0$ )

$$t_{k+1} - t_k = d_k \leq d, \quad \forall k \geq 0. \quad (4)$$

Given the synchronization scheme (1)–(3), the synchronization error is defined as  $r(t) = x(t) - z(t)$ , and we can have the following synchronization error system:

$$\dot{r}(t) = \mathcal{A}r(t) + \mathcal{B}r(t-h) + \mathcal{W}g(\mathcal{D}r(t), z(t)) - \mathcal{K}\mathcal{C}r(t_k), \quad \forall k, t \in [t_k, t_{k+1}), \quad (5)$$

where  $g(\mathcal{D}r(t), z(t)) = f(\mathcal{D}r(t) + \mathcal{D}z(t)) - f(\mathcal{D}z(t))$ . Let  $\mathcal{D} = [\mathcal{D}_1, \mathcal{D}_2, \dots, \mathcal{D}_m]^T$  with  $\mathcal{D}_s \in \mathbb{R}^n, s = 1, 2, \dots, m$ . As  $f(\cdot)$  belongs to sector  $[k_s^-, k_s^+]$ , it is easy to discover that for any  $s = 1, 2, \dots, m$  and  $\forall r, z, \mathcal{D}_s^T r \neq 0$

$$k_s^- \leq \frac{g_s(\partial_s^T r, z)}{\partial_s^T r} = \frac{f_s(\partial_s^T(r+z)) - f_s(\partial_s^T z)}{\partial_s^T r} \leq k_s^+ \tag{6}$$

Moreover, it is easily found from (6) that for any  $s = 1, 2, \dots, m$  and  $\forall r, z$

$$\begin{aligned} & [g_s(\partial_s^T r(t), z(t)) - k_s^- \partial_s^T r(t)] \\ & \times [g_s(\partial_s^T r(t), z(t)) - k_s^+ \partial_s^T r(t)] \leq 0. \end{aligned} \tag{7}$$

*Remark 1* In the condition (6),  $k_s^-$  and  $k_s^+$  can be allowed to be positive, negative or zero. As mentioned in [28–30], it describes the class of globally Lipschitz continuous and monotone nondecreasing nonlinear function when  $k_s^- = 0$  and  $k_s^+ > 0$ . And the class of globally Lipschitz continuous and monotone increasing nonlinear function can be described when  $k_s^- > 0$  and  $k_s^+ > 0$ . Therefore, this type of nonlinear function is clearly more general than both the usual sigmoid nonlinear function and the piecewise liner function, which is more advantageous to reduce the conservatism of the results.

In the paper, the following lemmas are used in deriving the criteria.

**Lemma 1** [51] *For a given matrix  $M > 0$ , given scalars  $a$  and  $b$  satisfying  $a < b$ , the following inequality holds for all continuously differentiable function  $r$  in  $[a, b] \rightarrow \mathbb{R}^n$ :*

$$\begin{aligned} & -\frac{(b-a)^2}{2} \int_a^b \int_\theta^b r^T(s) M r(s) ds d\theta \\ & \leq -\int_a^b \int_\theta^b r^T(s) ds M \int_a^b \int_\theta^b r(s) ds - 2\Theta_d^T M \Theta_d, \end{aligned}$$

where  $\Theta_d = -\int_a^b \int_\theta^b r(s) ds d\theta + \frac{3}{b-a} \int_a^b \int_\lambda^b \int_\theta^b r(s) ds d\theta d\lambda$ .

**Lemma 2** *For a given symmetric positive definite matrix  $R$ , arbitrary scalars  $0 \leq \alpha \leq 1$  and  $0 \leq \beta \leq 1$  ( $\alpha + \beta = 1$ ), and for differentiable signal  $r(t)$  in  $[0, h] \rightarrow \mathbb{R}^n$ , the following inequality holds:*

$$-\int_{t-h}^t \dot{r}^T(s) R \dot{r}(s) ds$$

$$\begin{aligned} & \leq - \begin{bmatrix} r(t) \\ r(t-h) \\ \int_{t-h}^t r(s) ds \end{bmatrix}^T \begin{bmatrix} \frac{4\beta}{h} & \frac{2\beta}{h} & \frac{-6\beta}{h^2} \\ \frac{2\beta}{h} & \frac{4-2\alpha}{h} & \frac{-6+4\alpha}{h^2} \\ \frac{-6\beta}{h^2} & \frac{-6+4\alpha}{h^2} & \frac{12-10\alpha}{h^3} \end{bmatrix} \\ & \otimes R \begin{bmatrix} r(t) \\ r(t-h) \\ \int_{t-h}^t r(s) ds \end{bmatrix}. \end{aligned}$$

*Proof* From the celebrated Jensen’s integral inequality [49] and Wirtinger integral inequality [50], for random scalars  $0 \leq \alpha \leq 1$  and  $0 \leq \beta \leq 1$  ( $\alpha + \beta = 1$ ), we can obtain the following integral inequality:

$$\begin{aligned} & -\int_{t-h}^t \dot{r}^T(s) R \dot{r}(s) ds \\ & = -\alpha \int_{t-h}^t \dot{r}^T(s) R \dot{r}(s) ds - \beta \int_{t-h}^t \dot{r}^T(s) R \dot{r}(s) ds \\ & \leq - \begin{bmatrix} r(t-h) \\ \int_{t-h}^t r(s) ds \end{bmatrix}^T \begin{bmatrix} \frac{2\alpha}{h} & \frac{-2\alpha}{h^2} \\ \frac{-2\alpha}{h^2} & \frac{2\alpha}{h^3} \end{bmatrix} \\ & \otimes R \begin{bmatrix} r(t-h) \\ \int_{t-h}^t r(s) ds \end{bmatrix} - \begin{bmatrix} r(t) \\ r(t-h) \\ \int_{t-h}^t r(s) ds \end{bmatrix}^T \\ & \begin{bmatrix} \frac{4\beta}{h} & \frac{2\beta}{h} & \frac{-6\beta}{h^2} \\ \frac{2\beta}{h} & \frac{4\beta}{h} & \frac{-6\beta}{h^2} \\ \frac{-6\beta}{h^2} & \frac{-6\beta}{h^2} & \frac{12\beta}{h^3} \end{bmatrix} \otimes R \begin{bmatrix} r(t) \\ r(t-h) \\ \int_{t-h}^t r(s) ds \end{bmatrix} \\ & = - \begin{bmatrix} r(t) \\ r(t-h) \\ \int_{t-h}^t r(s) ds \end{bmatrix}^T \begin{bmatrix} \frac{4\beta}{h} & \frac{2\beta}{h} & \frac{-6\beta}{h^2} \\ \frac{2\beta}{h} & \frac{4-2\alpha}{h} & \frac{-6+4\alpha}{h^2} \\ \frac{-6\beta}{h^2} & \frac{-6+4\alpha}{h^2} & \frac{12-10\alpha}{h^3} \end{bmatrix} \\ & \otimes R \begin{bmatrix} r(t) \\ r(t-h) \\ \int_{t-h}^t r(s) ds \end{bmatrix}. \end{aligned}$$

This completes the proof. □

*Remark 2* When  $\alpha = 0$  and  $\beta = 1$ , this integral inequality can be reduced to the celebrated Wirtinger integral inequality [50]. When  $\alpha = 1$  and  $\beta = 0$ , this integral inequality can become the well-known Jensen inequality [49]. It is worth mentioning that the existing inequalities become the special cases of our inequality, which is proved to be more sharper and should have a great potential in practice.

### 3 Main results

In this section, we will propose some new master-slave synchronization conditions of CDLSs by using sampled-data feedback control and a novel integral inequality.

For the sake of simplicity of matrix representation,  $e_i^T = [0, \dots, I, \dots, 0]$  ( $i = 1, \dots, 12$ ) and  $\tilde{e}_j^T = [0, \dots, I, \dots, 0]$  ( $j = 1, \dots, 4$ ) are defined as block entry matrices. The notations for some vectors and matrices are defined as follows

$$\begin{aligned}
 &0 < \alpha < 1, \beta = 1 - \alpha, 0 \leq x_1, x_2 \leq 1, \\
 &x_1 + x_2 = 1, x_3 > 0, \\
 &\vartheta > 0, \sigma = 1 - \delta, \Sigma_2 = [-I, \mathcal{A}, \mathcal{B}, \mathcal{W}, -\mathcal{H}\mathcal{C}], \\
 &\varpi_1(t) = \int_{t-\alpha h}^t r(s)ds, \quad \varpi_2(t) = \int_{t-h}^{t-\alpha h} r(s)ds, \\
 &\Sigma_1 = [\zeta, y, \eta]^T, \\
 &\varpi_3(t) = \int_{t-\alpha h}^t \int_{\theta}^t r(s)dsd\theta, \\
 &\varpi_4(t) = \int_{t-h}^t \int_{\theta}^t r(s)dsd\theta, \\
 &\xi^T(t) = [r^T(t), \dot{r}^T(t), r^T(t_k), r^T(t - \alpha h), \\
 &r^T(t - h), g^T(\mathcal{D}r(t), \\
 &z(t)), g^T(\mathcal{D}r(t - \alpha h), z(t - \alpha h)), \\
 &g^T(\mathcal{D}r(t - h), z(t - h)), \\
 &\varpi_1^T(t), \varpi_2^T(t), \varpi_3^T(t), \varpi_4^T(t)], \\
 &\varepsilon^T(t) = [r^T(t), r^T(t_k)], \\
 &\varphi(t) = [r^T(t), \dot{r}^T(t), r^T(t_k)]^T, \\
 &\Pi(x_1, x_2, x_3) = \begin{bmatrix} \frac{4x_2}{x_3} & \frac{2x_2}{x_3} & \frac{-6x_2}{x_3^2} \\ \frac{2x_2}{x_3} & \frac{4-2x_1}{x_3} & \frac{-6+4x_1}{x_3^2} \\ \frac{-6x_2}{x_3^2} & \frac{-6+4x_1}{x_3^2} & \frac{12-10x_1}{x_3^3} \end{bmatrix}, \\
 &\mathcal{E}(\vartheta) = \begin{bmatrix} \frac{3}{2} & 0 & \frac{-3}{\vartheta^2} \\ 0 & \frac{3}{\vartheta^2} & \frac{-6}{\vartheta^3} \\ \frac{-3}{\vartheta^2} & \frac{-6}{\vartheta^3} & \frac{18}{\vartheta^4} \end{bmatrix}, \\
 &\mathcal{H} = \begin{bmatrix} 2\delta(H_1)_s & -H_1 + H_2 \\ * & 2(-H_2 + \sigma H_1)_s \end{bmatrix}.
 \end{aligned}$$

**Theorem 1** For given scalars  $h > 0, d > 0, \delta, x, y, z, 0 < \alpha < 1, 0 \leq \mu_1, \mu_2 \leq 1, \mu_1 + \mu_2 =$

$1, 0 \leq \nu_1, \nu_2 \leq 1$  and  $\nu_1 + \nu_2 = 1$ , the master system (1) and the slave system (2) are globally asymptotically synchronous for all  $d_k \leq d$  if there exist matrices  $P > 0, \mathcal{X} > 0, R_i > 0$  ( $i = 1, 2, \dots, 6$ ),  $\Omega = \text{diag}\{\omega_1, \omega_2, \dots, \omega_m\} > 0, L = \text{diag}\{l_1, l_2, \dots, l_m\} > 0, Q_{ii} = \text{diag}\{q_{i1}, q_{i2}, \dots, q_{iim}\} > 0$  ( $i = 1, 2, 3; i = 1, 2$ ), and any appropriately dimensioned matrices  $\mathcal{H}, N, U, M = [M_1, M_2, M_3]$  and  $\hat{M}(\bar{d}) = [\bar{d}^{\frac{1}{2}}M_1, \bar{d}^{\frac{1}{2}}M_2, \bar{d}^{\frac{1}{2}}M_3, 0, 0, 0, 0, 0, 0, 0, 0, 0]$ , such that

$$\begin{aligned}
 &\Phi(d) = \begin{bmatrix} P + 2\delta d(H_1)_s & -dH_1 + dH_2 \\ * & 2d(-H_2 + \sigma H_1)_s \end{bmatrix}, \quad (8) \\
 &\Psi_1(\bar{d}) = \Xi_0 + \Xi_{01} + \Xi_1(\bar{d}) < 0, \quad (9) \\
 &\Psi_2(\bar{d}) = \begin{bmatrix} \Xi_0 + \Xi_{02} & \hat{M}^T(\bar{d}) \\ * & -\mathcal{X} \end{bmatrix} < 0, \quad \bar{d} = 0, d, \quad (10)
 \end{aligned}$$

where

$$\begin{aligned}
 \Xi_0 &= e_1 R_1 e_1^T + e_2 \left( \alpha h R_3 + \beta h R_4 + \frac{\alpha^4 h^2}{4} R_5 + \frac{h^2}{4} R_6 \right) e_2^T \\
 &\quad - e_4 (R_1 - R_2) e_4^T - e_5 R_2 e_5^T - [e_1, e_3] \mathcal{H} [e_1, e_3]^T \\
 &\quad - [e_1, e_4, e_9] \Pi(\mu_1, \mu_2, \alpha h) \otimes R_3 [e_1, e_4, e_9]^T \\
 &\quad - [e_4, e_5, e_{10}] \Pi(\nu_1, \nu_2, \beta h) \otimes R_4 [e_4, e_5, e_{10}]^T \\
 &\quad - [e_1, e_9, e_{11}] \mathcal{E}(\alpha h) \otimes R_5 [e_1, e_9, e_{11}]^T \\
 &\quad - [e_1, e_9 + e_{10}, e_{12}] \mathcal{E}(h) \otimes R_6 [e_1, e_9 + e_{10}, e_{12}]^T \\
 &\quad + 2 \left( e_1 P e_2^T + e_2 \mathcal{D}^T (\Omega - L) e_6 + e_1 \mathcal{D}^T [K^+ L \right. \\
 &\quad \left. - K^- \Omega] \mathcal{D} e_2 + [e_2, e_1, e_3] \Sigma_1 N \Sigma_2 [e_2, e_1, e_5, e_6, e_3]^T \right. \\
 &\quad \left. + [e_1, e_2, e_3] M^T [e_1 - e_3]^T \right)_s, \\
 \Xi_{01} &= -2 \left[ e_1 \mathcal{D}^T K^- Q_{11} K^+ \mathcal{D} e_1^T + e_4 \mathcal{D}^T K^- Q_{21} K^+ \mathcal{D} e_4^T \right. \\
 &\quad \left. + e_5 \mathcal{D}^T K^- Q_{31} K^+ \mathcal{D} e_5^T + e_6 Q_{11} e_6^T + e_7 Q_{21} e_7^T \right. \\
 &\quad \left. + e_8 Q_{31} e_8^T \right] + 2 \left( e_1 \mathcal{D}^T (K^- + K^+) Q_{11} e_6^T + e_4 \mathcal{D}^T \right. \\
 &\quad \left. \times (K^- + K^+) Q_{21} e_7^T + e_5 \mathcal{D}^T (K^- + K^+) Q_{31} e_8^T \right)_s, \\
 \Xi_{02} &= -2 \left[ e_1 \mathcal{D}^T K^- Q_{12} K^+ \mathcal{D} e_1^T + e_4 \mathcal{D}^T K^- Q_{22} K^+ \mathcal{D} e_4^T \right. \\
 &\quad \left. + e_5 \mathcal{D}^T K^- Q_{32} K^+ \mathcal{D} e_5^T + e_6 Q_{12} e_6^T + e_7 Q_{22} e_7^T \right. \\
 &\quad \left. + e_8 Q_{32} e_8^T \right] + 2 \left( e_1 \mathcal{D}^T (K^- + K^+) Q_{12} e_6^T + e_4 \mathcal{D}^T \right. \\
 &\quad \left. \times (K^- + K^+) Q_{22} e_7^T + e_5 \mathcal{D}^T (K^- + K^+) Q_{32} e_8^T \right)_s, \\
 \Xi_1(\bar{d}) &= 2 \left( \bar{d} [e_1, e_3] \mathcal{H} [e_2, 0]^T \right)_s + \bar{d} e_2 \mathcal{X} e_2^T.
 \end{aligned}$$

Moreover, the gain matrix of state estimator is given by  $\mathcal{K} = N^{-1}U$ .

*Proof* Consider the following LKF for the synchronization error system (5) ( $t \in [t_k, t_{k+1})$ ):

$$V(t) = V_1(t) + V_2(t) + V_3(t) + V_4(t) + V_5(t) + V_6(t), \tag{11}$$

where

$$V_1(t) = r^T(t)Pr(t) + (t_{k+1} - t)\varepsilon^T(t)\mathcal{H}\varepsilon(t),$$

$$V_2(t) = (t_{k+1} - t) \int_{t_k}^t \dot{r}^T(s)\mathcal{X}\dot{r}(s)ds,$$

$$V_3(t) = \int_{t-\alpha h}^t r^T(s)R_1r(s)ds + \int_{t-h}^{t-\alpha h} r^T(s)R_2r(s)ds,$$

$$V_4(t) = \int_{-\alpha h}^0 \int_{t+\theta}^t \dot{r}^T(s)R_3\dot{r}(s)dsd\theta + \int_{-h}^{-\alpha h} \int_{t+\theta}^t \dot{r}^T(s)R_4\dot{r}(s)dsd\theta,$$

$$V_5(t) = \frac{\alpha^2}{2} \int_{t-\alpha h}^t \int_{\lambda}^t \int_{\theta}^t \dot{r}^T(s)R_5\dot{r}(s)dsd\theta d\lambda + \frac{1}{2} \int_{t-h}^t \int_{\lambda}^t \int_{\theta}^t \dot{r}^T(s)R_6\dot{r}(s)dsd\theta d\lambda,$$

$$V_6(t) = 2 \sum_{s=1}^m \omega_s \int_0^{\partial_s^T r(t)} [g_s(\theta) - k_s^-\theta] d\theta + 2 \sum_{s=1}^m l_s \int_0^{\partial_s^T r(t)} [k_s^+\theta - g_s(\theta)] d\theta.$$

From the assumption, we know that  $V_2(t), V_3(t), V_4(t), V_5(t)$  and  $V_6(t)$  are positive. If  $V_1(t)$  is positive definite,  $V(t)$  is also positive definite. It is easy to verify that

$$\begin{aligned} V(t) &> V_1(t) \\ &= r^T(t)Pr(t) + (t_{k+1} - t)\varepsilon^T(t)\mathcal{H}\varepsilon(t) \\ &= \begin{bmatrix} r(t) \\ r(t_k) \end{bmatrix}^T \left( \begin{bmatrix} P & 0 \\ * & 0 \end{bmatrix} + (t_{k+1} - t)\mathcal{H} \right) \\ &\quad \times \begin{bmatrix} r(t) \\ r(t_k) \end{bmatrix} \\ &= \begin{bmatrix} r(t) \\ r(t_k) \end{bmatrix}^T \left( \frac{t - t_k}{d_k} \Phi(0) + \frac{t_{k+1} - t}{d_k} \Phi(d_k) \right) \\ &\quad \times \begin{bmatrix} r(t) \\ r(t_k) \end{bmatrix}, \end{aligned}$$

according to the equation

$$\Phi(d_k) = \frac{d_k}{d} \Phi(d) + \frac{d - d_k}{d} \Phi(0).$$

It follows from  $P > 0$  and (8) that the LKF  $V(t) > 0$ . It is noted that two  $(t_k, t_{k+1})$ -dependent terms  $V_1(t)$  and  $V_2(t)$ , are introduced in the constructed LKF (11), which make the best of the available information about the actual sampling pattern. In addition,  $V(t)$  is continuous on the whole interval  $[0, \infty]$  because  $t_k, t_{k+1}$ -dependent terms  $V_1(t)$  and  $V_2(t)$  vanish before and after the jump  $t_k$ .

Now let us calculate the time derivative of  $V(t)$  along the trajectory of the synchronization error system (5) which yields:

$$\begin{aligned} \dot{V}_1(t) &= 2r^T(t)P\dot{r}(t) - \varepsilon^T(t)\mathcal{H}\dot{\varepsilon}(t) \\ &\quad + 2(t_{k+1} - t)\varepsilon^T(t)\mathcal{H}\dot{\varepsilon}(t) \\ &= \xi^T(t) \left[ \frac{t_{k+1} - t}{d_k} \left[ 2 \left( e_1 P e_2^T + d_k [e_1, e_3] \mathcal{H} [e_2, 0]^T \right)_s \right. \right. \\ &\quad \left. \left. - [e_1, e_3] \mathcal{H} [e_1, e_3]^T \right] + \frac{t - t_k}{d_k} \left[ 2 \left( e_1 P e_2^T \right)_s \right. \right. \\ &\quad \left. \left. - [e_1, e_3] \mathcal{H} [e_1, e_3]^T \right] \right] \xi(t), \tag{12} \end{aligned}$$

$$\dot{V}_2(t) = (t_{k+1} - t)\dot{r}^T(t)\mathcal{X}\dot{r}(t) - \int_{t_k}^t \dot{r}^T(s)\mathcal{X}\dot{r}(s)ds. \tag{13}$$

Moreover, for an appropriately dimensioned matrix  $M = [M_1, M_2, M_3]$ , we can get the following inequality:

$$\int_{t_k}^t \begin{bmatrix} \varphi(t) \\ \dot{r}(s) \end{bmatrix}^T \begin{bmatrix} M^T \mathcal{X}^{-1} M & M^T \\ * & \mathcal{X} \end{bmatrix} \begin{bmatrix} \varphi(t) \\ \dot{r}(s) \end{bmatrix} ds \geq 0.$$

This implies,

$$\begin{aligned} \dot{V}_2(t) &\leq (t_{k+1} - t)\dot{r}^T(t)\mathcal{X}\dot{r}(t) + (t - t_k)\varphi^T(t)M^T \mathcal{X}^{-1} \\ &\quad \times M\varphi(t) + 2\varphi^T(t)M^T(r(t) - r(t_k)) \\ &= \xi^T(t) \left[ \frac{t_{k+1} - t}{d_k} \left[ d_k e_2 \mathcal{X} e_2^T + 2 \left( [e_1, e_2, e_3] M^T \right. \right. \right. \\ &\quad \left. \left. \times [e_1 - e_3]^T \right)_s \right] + \frac{t - t_k}{d_k} \left[ d_k [e_1, e_2, e_3] M^T \mathcal{X}^{-1} M \right. \\ &\quad \left. \times [e_1, e_2, e_3]^T + 2 \left( [e_1, e_2, e_3] M^T [e_1 - e_3]^T \right)_s \right] \right] \xi(t), \tag{14} \end{aligned}$$

$$\begin{aligned} \dot{V}_3(t) &= r^T(t)R_1r(t) - r^T(t - \alpha h)(R_1 - R_2)r(t - \alpha h) \\ &\quad - r^T(t - h)R_2r(t - h) \end{aligned}$$



$$\begin{aligned}
 &= \xi^T(t) \left[ \frac{t_{k+1}-t}{d_k} \left[ e_1 R_1 e_1^T \right. \right. \\
 &\quad \left. \left. - e_4(R_1 - R_2)e_4^T - e_5 R_2 e_5^T \right] + \frac{t-t_k}{d_k} \right. \\
 &\quad \left. \times \left[ e_1 R_1 e_1^T - e_4(R_1 - R_2)e_4^T - e_5 R_2 e_5^T \right] \right] \xi(t), \tag{15}
 \end{aligned}$$

$$\begin{aligned}
 \dot{V}_4(t) &= \dot{r}^T(t)(\alpha h R_3 + (1-\alpha)h R_4)\dot{r}(t) \\
 &\quad - \int_{t-\alpha h}^t \dot{r}^T(s) R_3 \dot{r}(s) ds \\
 &\quad - \int_{t-h}^{t-\alpha h} \dot{r}^T(s) R_4 \dot{r}(s) ds. \tag{16}
 \end{aligned}$$

From Lemma 2, for any positive variable parameters  $\mu_i$  and  $v_i$  ( $i = 1, 2$ ) satisfying  $\mu_1 + \mu_2 = 1$  and  $v_1 + v_2 = 1$ , we can have easily

$$\begin{aligned}
 &- \int_{t-\alpha h}^t \dot{r}^T(s) R_3 \dot{r}(s) ds \\
 &= -\mu_1 \int_{t-\alpha h}^t \dot{r}^T(s) R_3 \dot{r}(s) ds \\
 &\quad - \mu_2 \int_{t-\alpha h}^t \dot{r}^T(s) R_3 \dot{r}(s) ds \\
 &\leq - \begin{bmatrix} r(t) \\ r(t-\alpha h) \\ \int_{t-\alpha h}^t r(s) ds \end{bmatrix}^T \begin{bmatrix} \frac{4\mu_2}{\alpha h} & \frac{2\mu_2}{\alpha h} & \frac{-6\mu_2}{(\alpha h)^2} \\ \frac{2\mu_2}{\alpha h} & \frac{4-2\mu_1}{\alpha h} & \frac{-6+4\mu_1}{(\alpha h)^2} \\ \frac{-6\mu_2}{(\alpha h)^2} & \frac{-6+4\mu_1}{(\alpha h)^2} & \frac{12-10\mu_1}{(\alpha h)^3} \end{bmatrix} \\
 &\quad \otimes R_3 \begin{bmatrix} r(t) \\ r(t-\alpha h) \\ \int_{t-\alpha h}^t r(s) ds \end{bmatrix}, \tag{17}
 \end{aligned}$$

$$\begin{aligned}
 &- \int_{t-h}^{t-\alpha h} \dot{r}^T(s) R_4 \dot{r}(s) ds \\
 &= -v_1 \int_{t-h}^{t-\alpha h} \dot{r}^T(s) R_4 \dot{r}(s) ds - v_2 \int_{t-h}^{t-\alpha h} \dot{r}^T(s) R_4 \dot{r}(s) ds \\
 &\leq - \begin{bmatrix} r(t-\alpha_1 h) \\ r(t-h) \\ \int_{t-h}^{t-\alpha h} r(s) ds \end{bmatrix}^T \begin{bmatrix} \frac{4v_2}{\beta h} & \frac{2v_2}{\beta h} & \frac{-6v_2}{(\beta h)^2} \\ \frac{2v_2}{\beta h} & \frac{4-2v_1}{\beta h} & \frac{-6+4v_1}{(\beta h)^2} \\ \frac{-6v_2}{(\beta h)^2} & \frac{-6+4v_1}{(\beta h)^2} & \frac{12-10v_1}{(\beta h)^3} \end{bmatrix} \\
 &\quad \otimes R_4 \begin{bmatrix} r(t-\alpha h) \\ r(t-h) \\ \int_{t-h}^{t-\alpha h} r(s) ds \end{bmatrix}. \tag{18}
 \end{aligned}$$

Applying (17) and (18) to (16), we may gain

$$\begin{aligned}
 \dot{V}_4(t) &\leq \xi^T(t) \left[ \frac{t_{k+1}-t}{d_k} \left[ e_2(\alpha h R_3 + \beta h R_4) e_2^T \right. \right. \\
 &\quad \left. \left. - [e_1, e_4, e_9] \Pi(\mu_1, \mu_2, \alpha h) \otimes R_3 [e_1, e_4, e_9]^T \right. \right. \\
 &\quad \left. \left. - [e_4, e_5, e_{10}] \Pi(v_1, v_2, \beta h) \otimes R_4 [e_4, e_5, e_{10}]^T \right] \right] \xi(t)
 \end{aligned}$$

$$\begin{aligned}
 &+ \frac{t-t_k}{d_k} \left[ e_2(\alpha h R_3 + \beta h R_4) e_2^T - [e_1, e_4, e_9] \right. \\
 &\quad \left. \times \Pi(\mu_1, \mu_2, \alpha h) \otimes R_3 [e_1, e_4, e_9]^T - [e_4, e_5, e_{10}] \right. \\
 &\quad \left. \times \Pi(v_1, v_2, \beta h) \otimes R_4 [e_4, e_5, e_{10}]^T \right] \xi(t), \tag{19}
 \end{aligned}$$

$$\begin{aligned}
 \dot{V}_5(t) &= \dot{r}^T(t) \left( \frac{\alpha^4 h^2}{4} R_5 + \frac{h^2}{4} R_6 \right) \dot{r}(t) \\
 &\quad - \frac{\alpha^2}{2} \int_{t-\alpha h}^t \int_{\theta}^t \dot{r}^T(s) R_5 \dot{r}(s) ds d\theta \\
 &\quad - \frac{1}{2} \int_{t-h}^t \int_{\theta}^t \dot{r}^T(s) R_6 \dot{r}(s) ds d\theta. \tag{20}
 \end{aligned}$$

By using Lemma 1, we can get

$$\begin{aligned}
 &- \frac{\alpha^2}{2} \int_{t-\alpha h}^t \int_{\theta}^t \dot{r}^T(s) R_5 \dot{r}(s) ds d\theta \\
 &\leq - \begin{bmatrix} r(t) \\ \int_{t-\alpha h}^t r(s) ds \\ \int_{t-\alpha h}^t \int_{\theta}^t r(s) ds d\theta \end{bmatrix}^T \begin{bmatrix} \frac{3}{2} & 0 & \frac{-3}{(\alpha h)^2} \\ 0 & \frac{3}{(\alpha h)^2} & \frac{-6}{(\alpha h)^3} \\ \frac{-3}{(\alpha h)^2} & \frac{-6}{(\alpha h)^3} & \frac{18}{(\alpha h)^4} \end{bmatrix} \\
 &\quad \otimes R_5 \begin{bmatrix} r(t) \\ \int_{t-\alpha h}^t r(s) ds \\ \int_{t-\alpha h}^t \int_{\theta}^t r(s) ds d\theta \end{bmatrix}, \tag{21}
 \end{aligned}$$

$$\begin{aligned}
 &- \frac{1}{2} \int_{t-h}^t \int_{\theta}^t \dot{r}^T(s) R_6 \dot{r}(s) ds d\theta \\
 &\leq - \begin{bmatrix} r(t) \\ \int_{t-\alpha h}^t r(s) ds + \int_{t-h}^{t-\alpha h} r(s) ds \\ \int_{t-h}^t \int_{\theta}^t r(s) ds d\theta \end{bmatrix}^T \begin{bmatrix} \frac{3}{2} & 0 & \frac{-3}{h^2} \\ 0 & \frac{3}{h^2} & \frac{-6}{h^3} \\ \frac{-3}{h^2} & \frac{-6}{h^3} & \frac{18}{h^4} \end{bmatrix} \\
 &\quad \otimes R_6 \begin{bmatrix} r(t) \\ \int_{t-\alpha h}^t r(s) ds + \int_{t-h}^{t-\alpha h} r(s) ds \\ \int_{t-h}^t \int_{\theta}^t r(s) ds d\theta \end{bmatrix}. \tag{22}
 \end{aligned}$$

Applying (21) and (22) to (20), we can gain

$$\begin{aligned}
 \dot{V}_5(t) &\leq \xi^T(t) \left[ \frac{t_{k+1}-t}{d_k} \left[ e_2 \left( \frac{\alpha^4 h^2}{4} R_5 + \frac{h^2}{4} R_6 \right) e_2^T \right. \right. \\
 &\quad \left. \left. - [e_1, e_9, e_{11}] \mathcal{E}(\alpha h) \otimes R_5 [e_1, e_9, e_{11}]^T \right. \right. \\
 &\quad \left. \left. - [e_1, e_9 + e_{10}, e_{12}] \mathcal{E}(h) \right. \right. \\
 &\quad \left. \left. \otimes R_6 [e_1, e_9 + e_{10}, e_{12}]^T \right] \right. \\
 &\quad \left. + \frac{t-t_k}{d_k} \left[ e_2 \left( \frac{\alpha^4 h^2}{4} R_5 + \frac{h^2}{4} R_6 \right) e_2^T \right. \right. \\
 &\quad \left. \left. - [e_1, e_9, e_{11}] \times \mathcal{E}(\alpha h) \otimes R_5 [e_1, e_9, e_{11}]^T \right. \right. \\
 &\quad \left. \left. - [e_1, e_9 + e_{10}, e_{12}] \right. \right. \\
 &\quad \left. \left. \times \mathcal{E}(h) \otimes R_6 [e_1, e_9 + e_{10}, e_{12}]^T \right] \right] \xi(t), \tag{23}
 \end{aligned}$$

$$\begin{aligned} \dot{V}_6(t) &= 2 \sum_{s=1}^m (\omega_s - l_s) \mathfrak{D}_s^T \dot{r}(t) g_s \left( \mathfrak{D}_s^T r(t), z(t) \right) \\ &\quad + 2 \sum_{s=1}^m \mathfrak{D}_s^T \dot{r}(t) (l_s k_s^+ - \omega_s k_s^-) \mathfrak{D}_s^T r(t) \\ &= 2 \dot{r}^T(t) \mathcal{D}^T (\Omega - L) g(\mathcal{D}r(t), z(t)) \\ &\quad + 2 r^T(t) \mathcal{D}^T [K^+ L - K^- \Omega] \mathcal{D} \dot{r}(t) \\ &= \xi^T(t) \left[ 2 \frac{t_{k+1} - t}{d_k} \left( e_2 \mathcal{D}^T (\Omega - L) e_6^T \right. \right. \\ &\quad \left. \left. + e_1 \mathcal{D}^T [K^+ L - K^- \Omega] \mathcal{D} e_2^T \right)_s \right. \\ &\quad \left. + 2 \frac{t - t_k}{d_k} \left( e_2 \mathcal{D}^T (\Omega - L) e_6^T \right. \right. \\ &\quad \left. \left. + e_1 \mathcal{D}^T [K^+ L - K^- \Omega] \mathcal{D} e_2^T \right)_s \right] \xi(t). \end{aligned} \tag{24}$$

Next, for any scalars  $\zeta$ ,  $y$  and  $\eta$ , and arbitrary matrix  $N$  with appropriate dimensions, we can obtain

$$\begin{aligned} 0 &= 2[\dot{r}^T(t)\zeta + r^T(t)y + r^T(t_k)\eta]N[-\dot{r}(t) + \mathcal{A}r(t) \\ &\quad + \mathcal{B}r(t-h) + \mathcal{W}g(\mathcal{D}r(t), z(t)) - \mathcal{H}\mathcal{C}r(t_k)] \\ &= \xi^T(t) \left[ 2 \frac{t_{k+1} - t}{d_k} ([e_2, e_1, e_3] \Sigma_1 N \Sigma_2 \right. \\ &\quad \left. \times [e_2, e_1, e_5, e_6, e_3]^T)_s + 2 \frac{t - t_k}{d_k} \right. \\ &\quad \left. \times ([e_2, e_1, e_3] \Sigma_1 N \Sigma_2 [e_2, e_1, e_5, e_6, e_3]^T)_s \right] \xi(t). \end{aligned} \tag{25}$$

According to the Eq. (7), for any positive diagonal matrices  $Q_{1i} = \text{diag}\{q_{11i}, q_{12}, \dots, q_{1mi}\}$ ,  $Q_{2i} = \text{diag}\{q_{21i}, q_{22i}, \dots, q_{2mi}\}$ , and  $Q_{3i} = \text{diag}\{q_{31i}, q_{32i}, \dots, q_{3mi}\}$ ,  $i = 1, 2$ , we may have following inequalities

$$\begin{aligned} &- 2 \sum_{s=1}^m \left[ g_s \left( \mathfrak{D}_s^T r(t), z(t) \right) - k_s^- \mathfrak{D}_s^T r(t) \right] q_{1si} \\ &\quad \times \left[ g_s \left( \mathfrak{D}_s^T r(t), z(t) \right) - k_s^+ \mathfrak{D}_s^T r(t) \right] \geq 0, \tag{26} \\ &- 2 \sum_{s=1}^m \left[ g_s \left( \mathfrak{D}_s^T r(t - \alpha h), z(t - \alpha h) \right) \right. \\ &\quad \left. - k_s^- \mathfrak{D}_s^T r(t - \alpha h) \right] q_{2si} \times \left[ g_s \left( \mathfrak{D}_s^T r(t - \alpha h), \right. \right. \\ &\quad \left. \left. z(t - \alpha h) \right) - k_s^+ \mathfrak{D}_s^T r(t - \alpha h) \right] \geq 0, \tag{27} \\ &- 2 \sum_{s=1}^m \left[ g_s \left( \mathfrak{D}_s^T r(t - h), z(t - h) \right) \right. \end{aligned}$$

$$\begin{aligned} &\left. - k_s^- \mathfrak{D}_s^T r(t - h) \right] q_{3si} \times \left[ g_s \left( \mathfrak{D}_s^T r(t - h), \right. \right. \\ &\quad \left. \left. z(t - h) \right) - k_s^+ \mathfrak{D}_s^T r(t - h) \right] \geq 0. \end{aligned} \tag{28}$$

From Eqs. (26)–(28), we can get

$$\begin{aligned} \zeta_1(i, t) &= -2g^T(\mathcal{D}r(t), z(t))Q_{1i}g(\mathcal{D}r(t), z(t)) \\ &\quad + 2r^T(t)\mathcal{D}^T(K^- + K^+)Q_{1i}g(\mathcal{D}r(t), z(t)) \\ &\quad - 2r^T(t)\mathcal{D}^TK^-Q_{1i}K^+\mathcal{D}r(t) \geq 0, \\ \zeta_2(i, t) &= -2g^T(\mathcal{D}r(t - \alpha h), z(t - \alpha h)) \\ &\quad Q_{2i}g(\mathcal{D}r(t - \alpha h), z(t - \alpha h)) \\ &\quad + 2r^T(t - \alpha h)\mathcal{D}^T(K^- + K^+) \\ &\quad Q_{2i}g(\mathcal{D}r(t - \alpha h), z(t - \alpha h)) \\ &\quad - 2r^T(t - \alpha h)\mathcal{D}^TK^-Q_{2i}K^+\mathcal{D}r(t - \alpha h) \geq 0, \\ \zeta_3(i, t) &= -2g^T(\mathcal{D}r(t - h), z(t - h)) \\ &\quad Q_{3i}g(\mathcal{D}r(t - h), z(t - h)) \\ &\quad + 2r^T(t - h)\mathcal{D}^T(K^- + K^+) \\ &\quad Q_{3i}g(\mathcal{D}r(t - h), z(t - h)) \\ &\quad - 2r^T(t - h)\mathcal{D}^TK^-Q_{3i}K^+\mathcal{D}r(t - h) \geq 0. \end{aligned}$$

Then

$$\begin{aligned} &\frac{t_{k+1} - t}{d_k} \zeta_1(1, t) + \frac{t - t_k}{d_k} \zeta_1(2, t) \\ &= \xi^T(t) \left[ \frac{t_{k+1} - t}{d_k} \left[ -2e_6Q_{11}e_6^T \right. \right. \\ &\quad \left. \left. - 2e_1\mathcal{D}^TK^-Q_{11}K^+\mathcal{D}e_1^T \right. \right. \\ &\quad \left. \left. + 2 \left( e_1\mathcal{D}^T(K^- + K^+)Q_{11}e_6^T \right)_s \right] \right. \\ &\quad \left. + \frac{t - t_k}{d_k} \left[ -2e_6Q_{12}e_6^T - 2e_1\mathcal{D}^TK^-Q_{12}K^+\mathcal{D}e_1^T \right. \right. \\ &\quad \left. \left. + 2 \left( e_1\mathcal{D}^T(K^- + K^+)Q_{12}e_6^T \right)_s \right] \right] \xi(t) \geq 0, \end{aligned} \tag{29}$$

$$\begin{aligned} &\frac{t_{k+1} - t}{d_k} \zeta_2(1, t) + \frac{t - t_k}{d_k} \zeta_2(2, t) \\ &= \xi^T(t) \left[ \frac{t_{k+1} - t}{d_k} \left[ -2e_7Q_{21}e_7^T \right. \right. \\ &\quad \left. \left. - 2e_4\mathcal{D}^TK^-Q_{21}K^+\mathcal{D}e_4^T \right. \right. \\ &\quad \left. \left. + 2 \left( e_4\mathcal{D}^T(K^- + K^+)Q_{21}e_7^T \right)_s \right] \right. \\ &\quad \left. + \frac{t - t_k}{d_k} \left[ -2e_7Q_{22}e_7^T - 2e_4\mathcal{D}^TK^-Q_{22}K^+\mathcal{D}e_4^T \right. \right. \\ &\quad \left. \left. + 2 \left( e_4\mathcal{D}^T(K^- + K^+)Q_{22}e_7^T \right)_s \right] \right] \xi(t) \geq 0, \end{aligned} \tag{30}$$



$$\begin{aligned} & \frac{t_{k+1}-t}{d_k} \zeta_3(1, t) + \frac{t-t_k}{d_k} \zeta_3(2, t) \\ &= \xi^T(t) \left[ \frac{t_{k+1}-t}{d_k} \left[ -2e_8 Q_{31} e_8^T \right. \right. \\ & \quad \left. \left. - 2e_5 \mathcal{D}^T K^- Q_{31} K^+ \mathcal{D} e_5^T \right. \right. \\ & \quad \left. \left. + 2 \left( e_5 \mathcal{D}^T (K^- + K^+) Q_{31} e_8^T \right)_s \right] \right. \\ & \quad \left. + \frac{t-t_k}{d_k} \left[ -2e_8 Q_{32} e_8^T - 2e_5 \mathcal{D}^T K^- Q_{32} K^+ \mathcal{D} e_5^T \right. \right. \\ & \quad \left. \left. + 2 \left( e_5 \mathcal{D}^T (K^- + K^+) Q_{32} e_8^T \right)_s \right] \right] \xi(t) \geq 0. \end{aligned} \tag{31}$$

By adding the right-hand side of (25) and the left-hand side of (29)–(31) to  $V(t)$  and letting  $U = NK$ , we obtain from (12)–(24) that for  $t \in [t_k, t_{k+1})$

$$\dot{V}(t) \leq \xi^T(t) \left[ \frac{t_{k+1}-t}{d_k} \Psi_1(d_k) + \frac{t-t_k}{d_k} \hat{\Psi}_2(d_k) \right] \xi(t), \tag{32}$$

where

$$\begin{aligned} \hat{\Psi}_2(d_k) &= \Xi_0 + \Xi_{02} + d_k [e_1, e_2, e_3] M^T \mathcal{X}^{-1} \\ & \quad M [e_1, e_2, e_3]^T. \end{aligned}$$

It is noted that

$$\Psi_1(d_k) = \frac{d_k}{d} \Psi_1(d) + \frac{d-d_k}{d} \Psi_1(0), \tag{33}$$

and

$$\hat{\Psi}_2(d_k) = \frac{d_k}{d} \hat{\Psi}_2(d) + \frac{d-d_k}{d} \hat{\Psi}_2(0). \tag{34}$$

From (9) and (10), we can find that

$$\Psi_1(d_k) < 0, \quad \hat{\Psi}_2(0) < 0. \tag{35}$$

Based on Schur complement, we have from (10)

$$\hat{\Psi}_2(d) < 0, \tag{36}$$

which, in combination with (35) and (36), implies

$$\hat{\Psi}_2(d_k) < 0. \tag{37}$$

Thus, we obtain from (32), (35) and (37) that

$$\begin{aligned} \dot{V}(t) &\leq \xi^T(t) \left[ \frac{t_{k+1}-t}{d_k} \Psi_1(d_k) \right. \\ & \quad \left. + \frac{t-t_k}{d_k} \hat{\Psi}_2(d_k) \right] \xi(t) < 0, \end{aligned} \tag{38}$$

which ensures that the synchronization error system (5) is globally asymptotically stable. Therefore, master system (1) and slave system (2) achieve global asymptotical synchronization. This completes the proof.  $\square$

*Remark 3* Since  $\Phi(\bar{d}) = \frac{\bar{d}}{d} \Phi(d) + \frac{d-\bar{d}}{d} \Phi(0) > 0$ , then  $\Psi_1(\bar{d}) = \frac{\bar{d}}{d} \Psi_1(d) + \frac{d-\bar{d}}{d} \Psi_1(0) < 0$  and  $\hat{\Psi}_2(\bar{d}) = \frac{\bar{d}}{d} \hat{\Psi}_2(d) + \frac{d-\bar{d}}{d} \hat{\Psi}_2(0) < 0$ . LIMs (8), (9) and (10) are convex in  $d$ , so they are feasible for all  $\bar{d} \in (0, d]$ , where  $d$  is the upper bound of all sampling intervals.

*Remark 4* Unlike that term in [19,41,48], we construct a novel LKF with a  $\delta$ ,  $\sigma$ ,  $H_1$  and  $H_2$ -dependent term  $\mathcal{H}$ , which is a kind of augmented functional. When  $\delta = \sigma = \frac{1}{2}$ , this term is a special case of that one in [19,41,48]. Thus, the LKF used here is more general and desirable than those employed in [19,41,48]. Besides, for the use of  $\mathcal{H}$ -dependent term, the constraint conditions of the matrices in the LKF have been relaxed. In the above theorem, this constraint is replaced by a more relaxable condition (8) to keep  $V_1(t)$  positive definite. For these reasons, the use of this term for variable sampling can improve further the obtained condition.

*Remark 5* The information of the slope of the nonlinear function has been considered fully. The slopes  $k_s^-$  and  $k_s^+$  are applied to construct  $V_6(t)$  of the LKF, while the LKF chosen in [28–30] ignores this information.

We consider the following sampled-data master–slave synchronization scheme free of time delay:

$$\mathfrak{M}: \begin{cases} \dot{x}(t) = \mathcal{A}x(t) + \mathcal{W}f(\mathcal{D}x(t)), \\ \gamma(t) = \mathcal{C}x(t), \end{cases} \tag{39}$$

$$\mathfrak{S}: \begin{cases} \dot{z}(t) = \mathcal{A}z(t) + \mathcal{W}f(\mathcal{D}z(t)) + u(t), \\ \lambda(t) = \mathcal{C}z(t), \end{cases} \tag{40}$$

$$\mathfrak{C}: u(t) = \mathcal{K}(\gamma(t_k) - \lambda(t_k)), t \in [t_k, t_{k+1}), \tag{41}$$

which has been studied in [19,28–30,42,46]. Correspondingly, the synchronization error system (5) is written as the following ( $\forall k, t \in [t_k, t_{k+1})$ ):

$$\dot{r}(t) = \mathcal{A}r(t) + \mathcal{W}g(\mathcal{D}r(t), z(t)) - \mathcal{K}\mathcal{C}r(t_k), \tag{42}$$

and the LKF (11) is constructed as

$$V(t) = V_1(t) + V_2(t) + V_6(t), \quad t \in [t_k, t_{k+1}), \quad (43)$$

where  $V_1(t)$ ,  $V_2(t)$  and  $V_6(t)$  are given in (11). Based on Theorem 1, we have the following Theorem.

**Theorem 2** For given scalars  $d > 0$ ,  $\delta$ ,  $x$ ,  $y$  and  $z$ , the master system (1) and the slave system (2) are globally asymptotically synchronous for all  $d_k \leq d$  if there exist matrices  $P > 0$ ,  $\mathcal{X} > 0$ ,  $\Omega = \text{diag}\{\omega_1, \omega_2, \dots, \omega_m\} > 0$ ,  $L = \text{diag}\{l_1, l_2, \dots, l_m\} > 0$ ,  $Q_{1i} = \text{diag}\{q_{1i1}, q_{1i2}, \dots, q_{1im}\} > 0$ , ( $i = 1, 2$ ), and any appropriately dimensioned matrices  $\mathcal{H}$ ,  $N$ ,  $U$ ,  $M = [M_1, M_2, M_3]$  and  $\tilde{M}(\bar{d}) = [\bar{d}^{\frac{1}{2}}M_1, \bar{d}^{\frac{1}{2}}M_2, \bar{d}^{\frac{1}{2}}M_3, 0]$ , such that

$$\Phi(d) = \begin{bmatrix} P + 2\delta d(H_1)_s & -dH_1 + dH_2 \\ * & 2d(-H_2) + \sigma(H_1)_s \end{bmatrix}, \quad (44)$$

$$\tilde{\Psi}_1(\bar{d}) = \tilde{\Xi}_0 + \tilde{\Xi}_{01} + \tilde{\Xi}_1(\bar{d}) < 0, \quad (45)$$

$$\tilde{\Psi}_2(\bar{d}) = \begin{bmatrix} \tilde{\Xi}_0 + \tilde{\Xi}_{02} & \tilde{M}^T(\bar{d}) \\ * & -\mathcal{X} \end{bmatrix} < 0, \quad \bar{d} = 0, d, \quad (46)$$

where

$$\begin{aligned} \tilde{\Xi}_0 &= -[\tilde{e}_1, \tilde{e}_3]\mathcal{H}[\tilde{e}_1, \tilde{e}_3]^T \\ &\quad + 2\left(\tilde{e}_1 P \tilde{e}_2^T + \tilde{e}_2 \mathcal{D}^T(\Omega - L)\tilde{e}_2^T\right. \\ &\quad + \tilde{e}_1 \mathcal{D}^T[K^+L - K^- \Omega]\mathcal{D}\tilde{e}_2^T \\ &\quad + [\tilde{e}_2, \tilde{e}_1, \tilde{e}_3]\Sigma_1 N \Sigma_2 \times [\tilde{e}_2, \tilde{e}_1, \tilde{e}_4, \tilde{e}_3]^T \\ &\quad \left. + [\tilde{e}_1, \tilde{e}_2, \tilde{e}_3]M^T[\tilde{e}_1 - \tilde{e}_3]^T\right)_s, \\ \tilde{\Xi}_{01} &= -2[\tilde{e}_1 \mathcal{D}^T K^- Q_{11} K^+ \mathcal{D}\tilde{e}_1^T + \tilde{e}_4 Q_{11} e_4^T] \\ &\quad + 2\left(\tilde{e}_1 \mathcal{D}^T(K^- + K^+)Q_{11}\tilde{e}_4^T\right)_s, \\ \tilde{\Xi}_{02} &= -2[\tilde{e}_1 \mathcal{D}^T K^- Q_{12} K^+ \mathcal{D}\tilde{e}_1^T + \tilde{e}_4 Q_{12}\tilde{e}_4^T] \\ &\quad + 2\left(\tilde{e}_1 \mathcal{D}^T(K^- + K^+)Q_{12}\tilde{e}_4^T\right)_s, \\ \tilde{\Xi}_1(\bar{d}) &= 2\left(\bar{d}[\tilde{e}_1, \tilde{e}_3]\mathcal{H}[\tilde{e}_2, 0]^T\right)_s + \bar{d}\tilde{e}_2 \mathcal{X} \tilde{e}_2^T. \end{aligned}$$

Moreover, the gain matrix of state estimator is given by  $\mathcal{H} = N^{-1}U$ .

**Remark 6** Different from the existing approaches in [28–30], in order to obtain less conservative stabil-

ity conditions, we propose a novel integral inequality to deal with the integral terms  $\int_{t-\alpha h}^t \dot{r}^T(s)R_3\dot{r}(s)ds$  and  $\int_{t-h}^{t-\alpha h} \dot{r}^T(s)R_4\dot{r}(s)ds$ , which encompasses the celebrated Wirtinger’s integral inequality and Jensen’s inequality as two special cases by introducing four tuning parameters  $\mu_i$  and  $\nu_i$  ( $i = 1, 2$ ).

**Remark 7** Moreover, the above tuning parameters can coordinate well the relations between the weight coefficient of  $\int_{t-\alpha h}^t \dot{r}^T(s)R_3\dot{r}(s)ds$ ,  $r(t)$ ,  $r(t - \alpha h)$  and  $\int_{t-h}^t r(s)ds$ , and  $\int_{t-h}^{t-\alpha h} \dot{r}^T(s)R_4\dot{r}(s)ds$ ,  $r(t - \alpha h)$ ,  $r(t - h)$  and  $\int_{t-h}^{t-\alpha h} r(s)ds$ , which reduce more significantly the conservatism of stability criteria than the existing ones. Thus, this kind of treatment method has greater potential and practicality than the existing ones.

**Remark 8** In this paper, we construct a new LKF with two triple integral terms  $\int_{t-\alpha h}^t \int_{\lambda}^t \int_{\theta}^t \dot{r}^T(s)R_5\dot{r}(s)dsd\theta d\lambda$  and  $\int_{t-h}^t \int_{\lambda}^t \int_{\theta}^t \dot{r}^T(s)R_6\dot{r}(s)dsd\theta d\lambda$ , which are not applied in the existing papers [19,28–30,47,48]. Besides, by using a double integral form of WBII in [51], we can take fully the relationship between  $\int_{t-\alpha h}^t \int_{\theta}^t \dot{r}^T(s)R_5\dot{r}(s)dsd\theta$ ,  $r(t)$ ,  $\int_{t-\alpha h}^t r(s)ds$  and  $\int_{t-\alpha h}^t \int_{\theta}^t r(s)dsd\theta$ , and  $\int_{t-h}^t \int_{\theta}^t \dot{r}^T(s)R_6\dot{r}(s)dsd\theta$ ,  $r(t)$ ,  $\int_{t-\alpha h}^t r(s)ds$ ,  $\int_{t-h}^{t-\alpha h} r(s)ds$  and  $\int_{t-h}^t \int_{\theta}^t r(s)dsd\theta$  into consideration. Furthermore, one numerical simulation example of Chua’s circuit is given in this paper. It will be shown expressly that the new double integral form of WBII enhances further the feasible region of stability criterion by comparing maximum delay bounds with the results obtained in our paper.

**Remark 9** In many actual engineering and applications, the maximum allowable sampling period  $d$  is valuable and meaningful. Such as, set  $\rho = \frac{1}{d}$  in Theorem 1 with fixed values  $h$ ,  $\delta$  and  $\alpha$ , the optimal value can be obtained through following optimization procedure:

$$\begin{cases} \text{Minimize } \rho & \text{for } \mu_i, \nu_i \in [0, 1], \quad i = 1, 2, \\ \text{Respect to } & (8) - (10). \end{cases} \quad (47)$$

Inequality (47) is a convex optimization problem and can be obtained efficiently by using the MATLAB LMI Toolbox.

### 4 Numerical examples

In this section, three numerical simulation examples are given to illustrate the effectiveness of the main results derived earlier.

*Example 1* Consider the following delayed Chua’s circuit via sampled-data feedback control [28–30,42,46]. The equation of Chua’s circuit can be expressed as:

$$\begin{cases} \dot{x}_1(t) = a(x_2(t) - m_1x_1(t) + f(x_1(t))) - cx_1(t - h), \\ \dot{x}_2(t) = x_1(t) - x_2(t) + x_3(t) - cx_1(t - h), \\ \dot{x}_3(t) = -bx_2(t) + c(2x_1(t - h) - x_3(t - h)), \end{cases} \tag{48}$$

with nonlinear characteristic satisfying

$$f(x_1(t)) = 0.5(m_1 - m_0)(|x_1(t) + 1| - |x_1(t) - 1|),$$

belonging to sector  $[0, 1]$ , and parameters  $m_0 = -\frac{1}{7}$ ,  $m_1 = \frac{2}{7}$ ,  $a = 9$ ,  $b = 14.28$ ,  $c = 0.1$ , and the constant delay  $h = 1$ .

Obviously, the system can be rewritten as the Lur’e form with the following parameters:

$$\mathcal{A} = \begin{bmatrix} -am_1 - 1 & a & 0 \\ 1 & -2 & 1 \\ 0 & -b & -1 \end{bmatrix}, \quad \mathcal{B} = \begin{bmatrix} -c & 0 & 0 \\ -c & 0 & 0 \\ 2c & 0 & -c \end{bmatrix},$$

$$\mathcal{W} = \begin{bmatrix} -a(m_0 - m_1) \\ 0 \\ 0 \end{bmatrix}, \quad \mathcal{C} = \mathcal{D} = \begin{bmatrix} 1 \\ 0 \\ 0 \end{bmatrix}^T.$$

The initial conditions of the master and slave systems are chosen as  $x(0) = [0.2, 0.3, 0.2]^T$  and  $z(0) = [-0.3, -0.1, 0.4]^T$ ,  $t \in [-1, 0]$ . Figures 3 and 4 show the master system states  $x(t)$  and the slave system states  $z(t)$  with  $u(t) = 0$ , respectively.

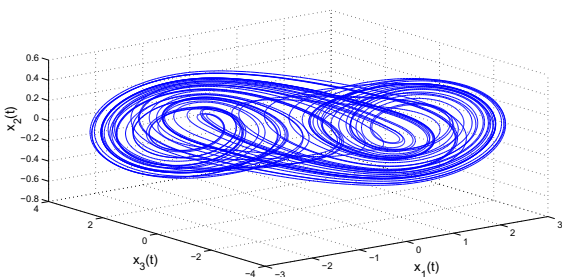


Fig. 3 State trajectories of master system

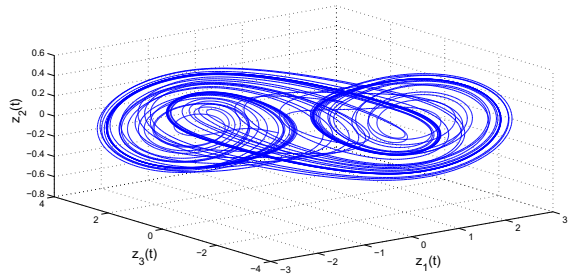


Fig. 4 State trajectories of slave system without  $u(t)$

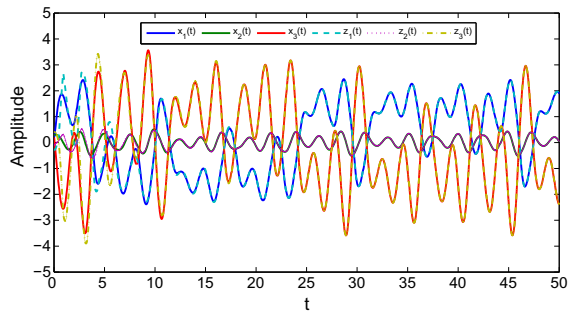


Fig. 5 State trajectories of master–slave system with  $u(t)$

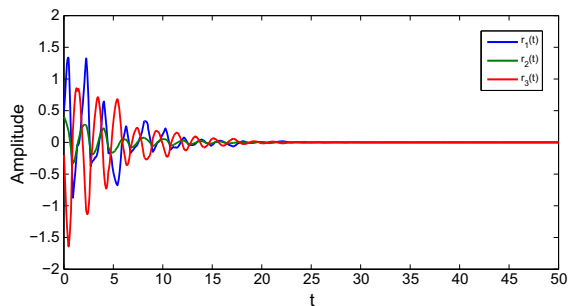
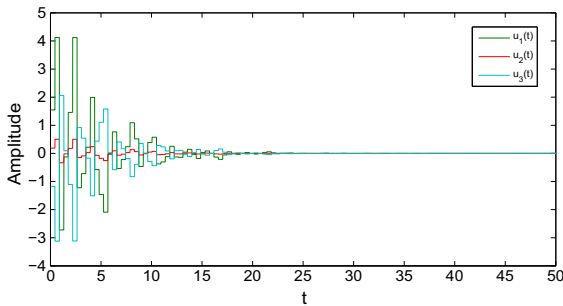


Fig. 6 State trajectories of synchronization error system with the sampling period  $d = 0.4369$

When  $\mu_1 = 0.5085$ ,  $\mu_2 = 0.4915$ ,  $\nu_1 = 0.5108$ ,  $\nu_2 = 0.4892$ ,  $\delta = 0.8176$ ,  $\alpha = 0.7948$ ,  $\zeta = 0.2886$ ,  $\gamma = -0.2428$  and  $\eta = 0.6232$ , by applying Theorem 1, the maximum value of the sampling period is  $d = 0.4369$ , and the corresponding sampled-data feedback control gain matrix is  $\mathcal{K} = [3.0960, 0.3779, -2.3436]^T$ .

Under the above  $\mathcal{K}$ , the responses of the state  $x(t)$  and  $z(t)$ , the error signal  $r(t)$  and control inputs  $u(t)$  are shown in Figs. 5, 6 and 7, respectively. Thus, we can synchronize successfully the master–slave systems by the proposed sampled-data controller. Moreover, by using Theorem 1, our obtained maximum sampling



**Fig. 7** State trajectories of the slave control input  $u(t)$

**Table 1** Comparison of maximum value of the sampling period of  $d$  in Example 1

Method	[28]	[29]	[30]	Theorem 1
$d$	0.3582	0.4355	0.4357	0.4369

period  $d$  and the detailed comparison with those in [28–30] are given in Table 1. From the Table 1, one can clearly see that the criterion in this letter provides a much less conservative result.

To demonstrate ulteriorly the reduced conservatism of the proposed condition, we choose  $c = 0$ ; that is, the time-delay Chua’s circuit (48) decreases to a Lur’e system free of time delay. This system has been studied in [28–30,42,46]. Applying Theorem 2, we have that the maximum value of the sampling period is 0.5218. When  $\delta = 0.4694$ ,  $\zeta = -0.9762$ ,  $y = -0.3258$  and  $\eta = -0.6756$ , the corresponding sampled-data feedback control gain matrix is  $\mathcal{K} = [2.6123, 0.2601, -1.6555]^T$ .

Therefore, our sampled-data control method is superior to the existing ones. The responses of the error signal  $r(t)$  and control inputs  $u(t)$  are shown in Figs. 8 and 9, where the initial conditions of the master and slave systems are chosen as  $x(0) = [0.7, 0.3, 0, 4]^T$  and  $z(0) = [-0.7, -0.5, 0.5]^T$ . The figures show that the controller achieves the master–slave synchronization. The comparisons on the allowable maximum value  $d$  are given in Table 2. The result illustrates that the sampled-data controller derived by the proposed criterion can achieve the synchronization of the master–slave systems under a larger sampling period.

**Example 2** Consider the master–slave systems in (39)–(41) with the following parameters [28,47,48]:

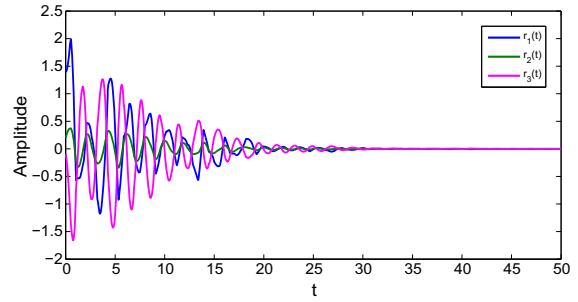


**Fig. 8** State trajectories of synchronization error system with the sampling period  $d = 0.5218$  for  $c = 0$

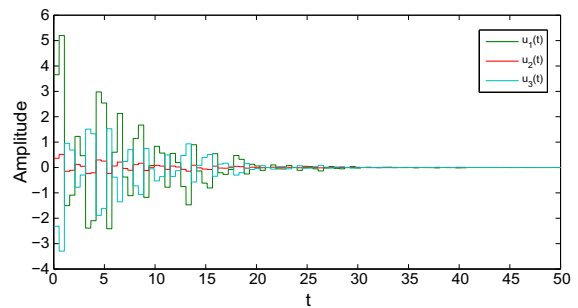


**Fig. 9** State trajectories of the slave control input  $u(t)$  for  $c = 0$

**Table 2** Comparison of maximum value of the sampling period of  $d$  for  $c = 0$  in Example 1

Method	[42]	[28]	[46]
$d$	0.3914	0.3981	0.4800
Method	[29]	[30]	Theorem 1
$d$	0.5144	0.5147	0.5218

$$\mathcal{A} = \begin{bmatrix} -1 & 0 & 0 \\ 0 & -1 & 0 \\ 0 & 0 & -1 \end{bmatrix}, \mathcal{W} = \begin{bmatrix} 1.2 & -1.6 & 0 \\ 1.24 & 1 & 0.9 \\ 0 & 2.2 & 1.5 \end{bmatrix},$$

$$\mathcal{C} = \mathcal{D} = I.$$

which implies that the Lur’e system reduces to a neural network with three neurons. Furthermore, the neuron activation functions  $f_s(x_s(t)) = 0.5(|x_s(t) + 1| - |x_s(t) - 1|)$ ,  $s = 1, 2, 3$ , and thus  $k_1^- = k_2^- = k_3^- = 0$  and  $k_1^+ = k_2^+ = k_3^+ = 1$ .

The initial states of the master and slave systems are chosen as  $x(0) = [0.4, 0.3, 0.8]^T$  and  $z(0) = [0.2, 0.4, 0.9]$ , respectively. The trajectories of the mas-

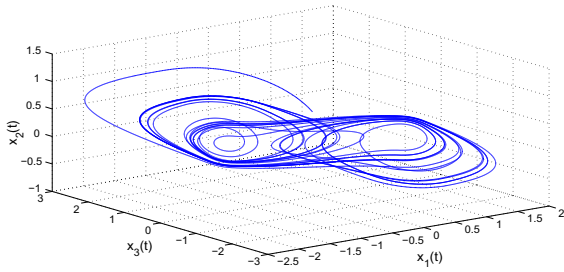


**Fig. 10** State trajectories of master system

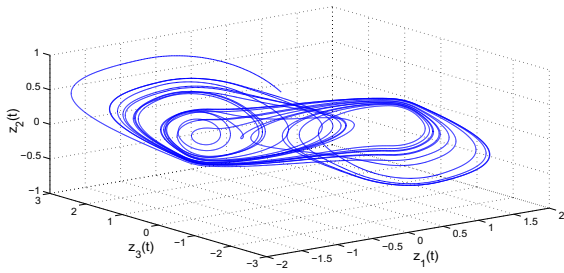


**Fig. 11** State trajectories of slave system without  $u(t)$

ter system and slave system with  $u(t) = 0$  are shown in Figs. 10 and 11, respectively.

When  $\delta = 0.6324, \zeta = -0.8049, y = -0.4430$  and  $\eta = 0.0938$ , based on Theorem 1, the maximum value of the sampling period is  $d = 0.3818$ , and the corresponding sampled-data feedback control gain matrix is

$$\mathcal{H} = \begin{bmatrix} 2.0123 & -1.9221 & 0.1277 \\ 1.6062 & 1.8970 & 0.8669 \\ 0.3166 & 1.6856 & 2.6986 \end{bmatrix}.$$

The responses of the state  $x(t)$  and  $z(t)$ , the error signal  $r(t)$  and control inputs  $u(t)$  are shown in Figs. 12, 13 and 14 for system (39)–(41) with the sampling period of 0.3818. We can observe that the controller achieves the master–slave synchronization. The maximum sampling period bound of this paper and that of [28, 47, 48] is shown in Table 3. The result declares clearly that the obtained sampled-data controller can achieve the synchronization of the master–slave system under a longer sampling period.

*Example 3* Consider the master–slave synchronization of two unidirectionally coupled Chua’s circuits via sampled-data feedback control [19].

The master system is given by

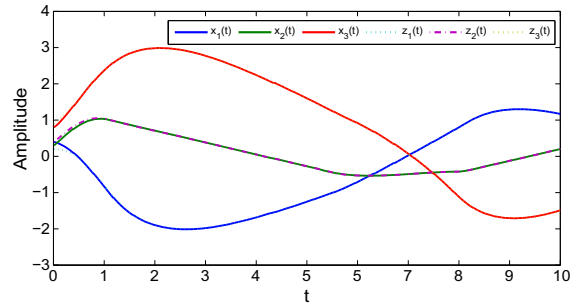


**Fig. 12** State trajectories of master–slave system with  $u(t)$

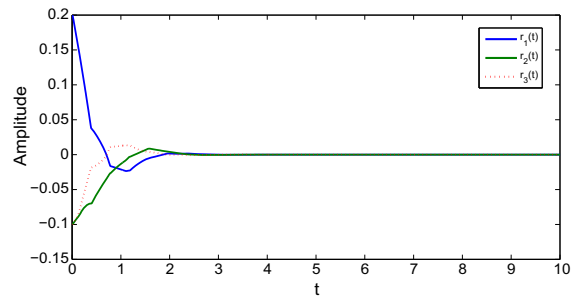


**Fig. 13** State trajectories of synchronization error system with the sampling period  $d = 0.3818$  for  $c = 0$

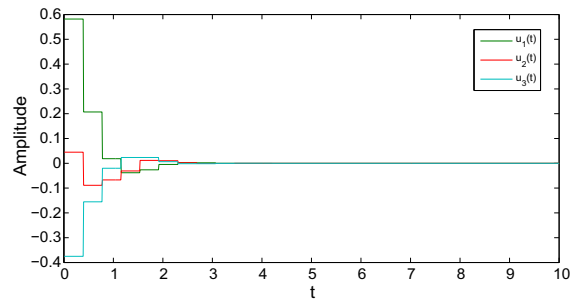


**Fig. 14** State trajectories of the slave control input  $u(t)$  for  $c = 0$

**Table 3** Comparison of maximum value of the sampling period of  $d$  in Example 2

Method	[47]	[48]	[28]	Theorem 2
$d$	0.1732	0.3212	0.3687	0.3818

$$\begin{cases} \dot{x}_1(t) = \alpha(x_2(t) - h(x_1(t))), \\ \dot{x}_2(t) = x_1(t) - x_2(t) + x_3(t), \\ \dot{x}_3(t) = -\beta x_2(t), \\ \dot{x}_4(t) = \alpha(x_5(t) - h(x_4(t))), \\ \dot{x}_5(t) = x_4(t) - x_5(t) + x_6(t) + G(x_5(t) - x_2(t)), \\ \dot{x}_6(t) = -\beta x_5(t), \end{cases} \quad (49)$$

with nonlinear characteristic satisfying ( $i = 1, 4$ )

$$h(x_i(t)) = l_1 x_i(t) + 0.5(l_0 - l_1)(|x_i(t)| + c) - |x_i(t) - c|,$$

belonging to a sector  $[0, 1]$ , and parameters  $l_0 = -\frac{1}{7}$ ,  $l_1 = \frac{2}{7}$ ,  $\alpha = 9$ ,  $\beta = 14.28$ ,  $c = 1$  and  $G = 0.01$ . The system can be represented in the Lur'e form with

$$\mathcal{A} = \begin{bmatrix} -\alpha l_1 & \alpha & 0 & 0 & 0 & 0 \\ 1 & -1 & 1 & 0 & 0 & 0 \\ 0 & -\beta & 0 & 0 & 0 & 0 \\ 0 & 0 & 0 & -\alpha l_1 & \alpha & 0 \\ 0 & -G & 0 & 1 & -1 + G & 1 \\ 0 & 0 & 0 & 0 & -\beta & 0 \end{bmatrix},$$

$$\mathcal{W} = \begin{bmatrix} -\alpha(l_0 - l_1) & 0 \\ 0 & 0 \\ 0 & 0 \\ 0 & -\alpha(l_0 - l_1) \\ 0 & 0 \\ 0 & 0 \end{bmatrix},$$

$$\mathcal{C} = \mathcal{D} = \begin{bmatrix} 1 & 0 \\ 0 & 0 \\ 0 & 0 \\ 0 & 1 \\ 0 & 0 \\ 0 & 0 \end{bmatrix}^T,$$

The slave system is considered with the same parameters as the master system studied in [19]. Applying the method proposed in [19], the maximum value of the upper bound is  $d = 0.25$ , while using Theorem 2 with  $\delta = 0.4218$ ,  $\zeta = 0.8315$ ,  $y = 0.5844$  and  $\eta = 0.9190$  given in this paper, the maximum value of the upper bound  $d$  that allows the synchronization of the master and slave systems is 0.26, and the corresponding sampled-data feedback control gain matrix is

$$\mathcal{K} = \begin{bmatrix} 4.9685 & 0.8770 & -3.3940 & -0.0022 & -0.0020 & 0.0055 \\ -0.0004 & -0.0000 & 0.0025 & 4.9706 & 0.8796 & -3.4019 \end{bmatrix}.$$

The initial values of master and slave systems are assumed to be  $x(0) = [0.1, 0.2, 0.3, 0.4, 0.5, 0.6]^T$  and  $z(0) = [-0.8, -0.6, -0.4, -0.2, 0, 0.2]^T$ , respectively. The trajectories of the master system and slave system with  $u(t) = 0$  are shown in Figs. 15 and 16, respectively. Moreover, the responses of the state  $x(t)$  and  $z(t)$ , the error signal  $r(t)$  and control inputs  $u(t)$

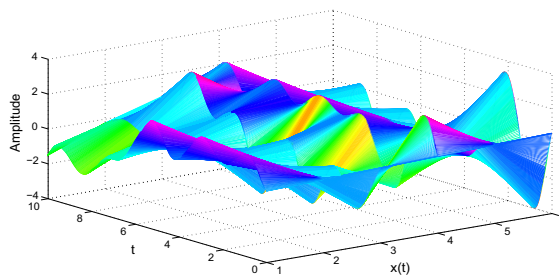


Fig. 15 State trajectories of master system on the space

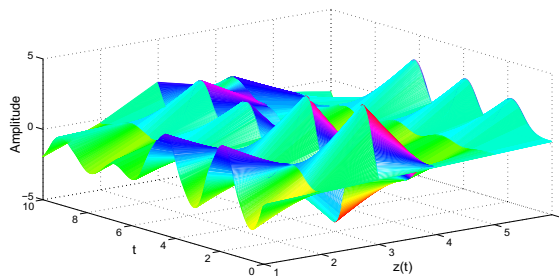


Fig. 16 State trajectories of slave system without  $u(t)$  on the space

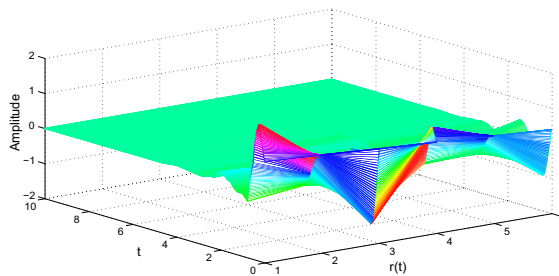


Fig. 17 State trajectories of synchronization error system with the sampling period  $d = 0.26$  on the space

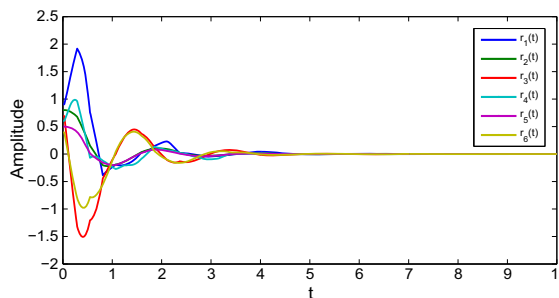
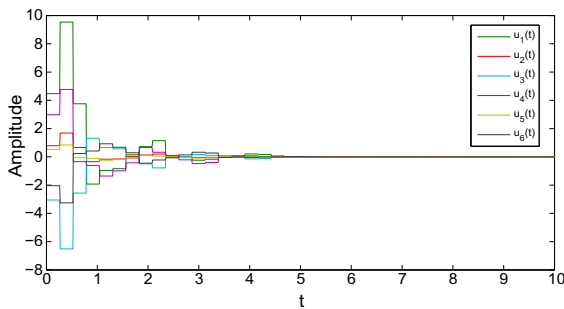


Fig. 18 State trajectories of synchronization error system with the sampling period  $d = 0.26$

are shown in Figs. 17, 18 and 19 for the systems (39)–(41) with the sampling period of 0.26, which demonstrates that the control law can guarantee the asymptot-





**Fig. 19** State trajectories of the slave control input  $u(t)$

ical synchronization of the master–slave system. Thus, it is clear to show that our approach is more effective than the recently reported one.

## 5 Conclusions

In this paper, the problem of master–slave synchronization of chaotic Lur’e systems with or without delays has been investigated by using sampled-data control method. A novel integral inequality is developed for the synchronization error systems by introducing new adjustable parameters, which is proved to be more tighter to estimate the bounds of the integral terms than the existing ones. Besides, a new and continuous LKF is constructed by taking full advantage of all kinds of available information. Thus, several less conservative synchronization criteria are obtained via a more general delay–partition approach. Furthermore, the desired feedback sampled-data controller is achieved by using a double integral form of WBII, which can provide a longer sampling period in realizing synchronization compared with the existing results. Finally, the feasibility and effectiveness of the proposed methods have been demonstrated via three numerical examples with simulations of typical Chua’s circuit. The foregoing methods may be potentially useful for further study of chaotic Lur’e systems with varying time delay. Meanwhile, it is expected that these approaches can be further used for other time-delay systems.

### Compliance with ethical standards

**Conflict of interest** The authors declare that there is no conflict of interests regarding the publication of this paper.

## References

1. Wu, Z., Shi, P., Su, H., Chu, J.: Local synchronization of chaotic neural networks with sampled-data and saturating actuators. *IEEE Trans. Cybern.* **44**, 2635–2645 (2014)
2. Zhang, D., Cai, W., Wang, Q.: Mixed  $H_\infty$  and passivity based state estimation for fuzzy neural networks with Markovian-type estimator gain change. *Neurocomputing* **139**, 321–327 (2014)
3. Zhang, D., Yu, L.: Exponential state estimation for Markovian jumping neural networks with time-varying discrete and distributed delays. *Neural Netw.* **35**, 103–111 (2012)
4. Wu, Z., Shi, P., Su, H., Chu, J.: Sampled-data exponential synchronization of complex dynamical networks with time-varying coupling delay. *IEEE Trans. Neural Netw. Learn. Syst.* **24**, 1177–1186 (2013)
5. Liu, Y., Lee, S.: Improved results on sampled-data synchronization of complex dynamical networks with time-varying coupling delay. *Nonlinear Dyn.* **81**, 931–938 (2015)
6. Shen, H., Park, J., Wu, Z., Zhang, Z.: Finite-time  $H_\infty$  synchronization for complex networks with semi-Markov jump topology. *Commun. Nonlinear Sci. Numer. Simul.* **24**, 40–51 (2015)
7. Li, K., Yu, W., Ding, Y.: Successive lag synchronization on nonlinear dynamical networks via linear feedback control. *Nonlinear Dyn.* **80**, 421–430 (2015)
8. Liu, J., Liu, S., Yuan, C.: Adaptive complex modified projective synchronization of complex chaotic (hyperchaotic) systems with uncertain complex parameters. *Nonlinear Dyn.* **79**, 1035–1047 (2015)
9. Liu, J., Liu, S., Zhang, F.: A novel four-wing hyperchaotic complex system and its complex modified hybrid projective synchronization with different dimensions. *Abstr. Appl. Anal.* (2014). doi:[10.1155/2014/257327](https://doi.org/10.1155/2014/257327)
10. Liu, J., Liu, S., Yuan, C.: Modified generalized projective synchronization of fractional-order chaotic Lü systems. *Adv. Differ. Equ.* (2013). doi:[10.1186/1687-1847-2013-374](https://doi.org/10.1186/1687-1847-2013-374)
11. Liu, J.: Complex modified hybrid projective synchronization of different dimensional fractional-order complex chaos and real hyper-chaos. *Entropy* **16**, 6195–6211 (2014)
12. Theesar, S., Balasubramaniam, P.: Secure communication via synchronization of Lur’e systems using sampled-data controller. *Circuits Syst. Signal Process.* **33**, 37–52 (2014)
13. Yin, C., Zhong, S., Chen, W.: Design PD controller for master–slave synchronization of chaotic Lur’e systems with sector and slope restricted nonlinearities. *Commun. Nonlinear Sci. Numer. Simul.* **16**, 1632–1639 (2011)
14. Wang, T., Zhou, W., Zhao, S., Yu, W.: Robust master–slave synchronization for general uncertain delayed dynamical model based on adaptive control scheme. *ISA Trans.* **53**, 335–340 (2014)
15. Li, X., Rakkiyappan, R.: Impulsive controller design for exponential synchronization of chaotic neural networks with mixed delays. *Commun. Nonlinear Sci. Numer. Simul.* **18**, 1515–1523 (2013)
16. Li, X., Song, S.: Research on synchronization of chaotic delayed neural networks with stochastic perturbation using impulsive control method. *Commun. Nonlinear Sci. Numer. Simul.* **19**, 3892–3900 (2014)



17. He, W., Qian, F., Han, Q., Cao, J.: Synchronization error estimation and controller design for delayed Lur'e systems with parameter mismatches. *IEEE Trans. Neural Netw. Learn. Syst.* **23**, 1551–1562 (2012)
18. Wu, Z., Shi, P., Su, H., Lu, R.: Dissipativity-based sampled-data fuzzy control design and its application to truck-trailer system. *IEEE Trans. Fuzzy Syst.* (2014). doi:[10.1109/TFUZZ.2014.2374192](https://doi.org/10.1109/TFUZZ.2014.2374192)
19. Wu, Y., Su, H., Wu, Z.: Asymptotical synchronization of chaotic Lur'e systems under time-varying sampling. *Circuits Syst. Signal Process.* **33**, 699–712 (2014)
20. Chen, W., Wei, D., Lu, X.: Global exponential synchronization of nonlinear time-delay Lur'e systems via delayed impulsive control. *Commun. Nonlinear Sci. Numer. Simul.* **19**, 3298–3312 (2014)
21. Rakkiyappan, R., Dharani, S., Zhu, Q.: Synchronization of reaction-diffusion neural networks with time-varying delays via stochastic sampled-data controller. *Nonlinear Dyn.* **79**, 485–500 (2015)
22. Ge, C., Hua, C.C., Guan, X.P.: Master-slave synchronization criteria of Lur'e systems with time-delay feedback control. *Appl. Math. Comput.* **244**, 895–902 (2014)
23. Han, Q.: On designing time-varying delay feedback controllers for master-slave synchronization of Lur'e systems. *IEEE Trans. Circuits Syst. II. Exp. Briefs* **70**, 1573–1583 (2012)
24. Qin, H., Ma, J., Jin, W., Wang, C.: Dynamics of electric activities in neuron and neurons of network induced by autapses. *Sci. China Technol. Sci.* **57**, 936–946 (2014)
25. Qin, H., Ma, J., Wang, C., Tong, C.: Autapse-induced target wave, spiral wave in regular network of neurons. *Sci. China Phys. Mech. Astron.* **57**, 1918–1926 (2014)
26. Shi, K., Zhu, H., Zhong, S., Zeng, Y., Zhang, Y.: New stability analysis for neutral type neural networks with discrete and distributed delays using a multiple integral approach. *J. Frankl. Inst.* **352**, 155–176 (2015)
27. Zeng, H., Park, J., Xia, J., Xiao, S.: Improved delay-dependent stability criteria for T-S fuzzy systems with time-varying delay. *Appl. Math. Comput.* **235**, 492–501 (2014)
28. Wu, Z., Shi, P., Su, H., Chu, J.: Sampled-data synchronization of chaotic Lur'e systems with time delays. *IEEE Trans. Neural Netw. Learn. Syst.* **24**, 410–420 (2013)
29. Hua, C., Ge, C., Guan, X.: Synchronization of chaotic Lur'e systems with time delays using sampled-data control. *IEEE Trans. Neural Netw. Learn. Syst.* (2014)
30. Ge, C., Zhang, W., Li, W., Sun, X.: Improved stability criteria for synchronization of chaotic Lur'e systems using sampled-data control. *Neurocomputing* **151**, 215–222 (2015)
31. Wu, Z., Shi, P., Su, H., Chu, J.: Sampled-data fuzzy control of chaotic systems based on a T-S fuzzy model. *IEEE Trans. Fuzzy Syst.* **22**, 153–163 (2014)
32. Wang, Z., Wu, H.: On fuzzy sampled-data control of chaotic systems via a time-dependent Lyapunov functional approach. *IEEE Trans. Cybern.* **45**, 819–828 (2015)
33. Wang, Z., Wu, H.: Synchronization of chaotic systems using fuzzy impulsive control. *Nonlinear Dyn.* **78**, 729–742 (2014)
34. Theesar, S., Banerjee, S., Balasubramaniam, P.: Synchronization of chaotic systems under sampled-data control. *Nonlinear Dyn.* **70**, 1977–1987 (2012)
35. Li, L., Yang, Y.: On sampled-data control for stabilization of genetic regulatory networks with leakage delays. *Neurocomputing* **149**, 1225–1231 (2015)
36. Xiao, X., Zhou, L., Zhang, Z.: Synchronization of chaotic Lur'e systems with quantized sampled-data controller. *Commun. Nonlinear Sci. Numer. Simul.* **19**, 2039–2047 (2014)
37. Zhang, X., Han, Q.: Event-based  $H_\infty$  filtering for sampled-data systems. *Automatica* **51**, 55–69 (2015)
38. Seuret, A.: A novel stability analysis of linear systems under asynchronous samplings. *Automatica* **48**, 177–182 (2012)
39. Zhu, X., Chen, B., Yue, D., Wang, Y.: An improved input delay approach to stabilization of fuzzy systems under variable sampling. *IEEE Trans. Fuzzy Syst.* **20**, 330–341 (2012)
40. Fridmana, E., Seuret, A., Richard, J.: Robust sampled-data stabilization of linear systems: an input delay approach. *Automatica* **40**, 1441–1446 (2004)
41. Fridman, E.: A refined input delay approach to sampled-data control. *Automatica* **46**, 421–427 (2010)
42. Chen, W., Wang, Z., Lu, X.: On sampled-data control for master-slave synchronization of chaotic Lur'e systems. *IEEE Trans. Circuits Syst. II. Exp. Briefs* **59**, 151–159 (2012)
43. Wu, Z., Shi, P., Su, H., Chu, J.: Stochastic synchronization of markovian jump neural networks with time-varying delay using sampled data. *IEEE Trans. Cybern.* **43**, 1–11 (2013)
44. Liu, Y., Lee, S.: Sampled-data synchronization of chaotic Lur'e systems with stochastic sampling. *Circuits Syst. Signal Process.* (2015). doi:[10.1007/s00034-015-0032-6](https://doi.org/10.1007/s00034-015-0032-6)
45. Ge, C., Li, Z., Huang, X., Shi, C.: New globally asymptotical synchronization of chaotic systems under sampled-data controller. *Nonlinear Dyn.* **78**, 2409–2419 (2014)
46. Zhang, C., Jiang, L., He, Y., Wu, Q., Wu, M.: Asymptotical synchronization for chaotic Lur'e systems using sampled-data control. *Commun. Nonlinear Sci. Numer. Simul.* **18**, 2743–2751 (2013)
47. Zhang, C., He, Y., Wu, M.: Exponential synchronization of neural networks with time-varying mixed delays and sampled-data. *Neurocomputing* **74**, 265–273 (2010)
48. Wu, Z., Shi, P., Su, H., Chu, J.: Exponential synchronization of neural networks with discrete and distributed delays under time-varying sampling. *IEEE Trans. Neural Netw. Learn. Syst.* **23**(9), 1368–1375 (2012)
49. Liu, Z., Yu, L., Xu, D.: Vector Wirtinger-type inequality and the stability analysis of delayed neural network. *Commun. Nonlinear Sci. Numer. Simul.* **18**, 1246–1257 (2013)
50. Seuret, A., Gouaisbaut, F.: Wirtinger-based integral inequality: application to time-delay systems. *Automatica* **49**, 2860–2866 (2013)
51. Park, M., Kwon, O., Park, J., Lee, S., Chad, E.: Stability of time-delay systems via Wirtinger-based double integral inequality. *Automatica* **55**, 204–208 (2015)